

# Short-Range Order in a Flat Two-Dimensional Fermi Surface

Eberth Corrêa, Hermann Freire, and A. Ferraz

Laboratório de Supercondutividade,  
Centro Internacional de Física da Materia Condensada,  
Universidade de Brasília – Brasília, Brazil  
(Dated: March 23, 2024)

We present the two-loop renormalization group (RG) calculations of all the susceptibilities associated with the two-dimensional flat Fermi surface with rounded corners (FS). Our approach follows our fermionic field theory RG method presented in detail earlier on. In one-loop order our calculation reproduces the results obtained previously by other RG schemes. All susceptibilities diverge at some energy scale and the antiferromagnetic SDW correlations produce indeed the dominant instability in the physical system. In contrast, in two-loop order, for a given initial set of values of coupling constant regime only one of the susceptibilities at a time seems to diverge.

PACS numbers: 71.10.Hf, 71.10.Pm, 71.27.+a

## I. INTRODUCTION

In the last decades there have been important developments in both experiment and theory which resulted in a better understanding of the high temperature superconductors. One typical characteristic of those compounds is their extreme sensitivity with doping. At half-filling the cuprates are Mott insulators. However, at very low hole doping, as soon as the antiferromagnetic ordering is destroyed those materials are turned into the pseudogap phase<sup>1,2,3,4</sup>.

From the start Anderson<sup>5</sup> argued that the Hubbard model (HM), which considers only short-range interactions, describes qualitatively well the electronic properties of the high- $T_c$  superconductors. In the one-dimensional case (1D) this model captures the main features displaying the existence of the Luttinger liquid for  $U > 0$ , spin-charge separation, as well as a Mott insulating regime. There is no exact solution for the HM in  $D > 1$ . Moreover successful methods in  $D = 1$  such as bosonization<sup>6</sup> and the Bethe ansatz<sup>7</sup> are either inapplicable or simply much too hard to implement in higher dimensions. One approach which is equally successful in both one and higher dimensions is the renormalization group (RG) method. Different RG schemes are already available to describe strongly interacting fermions in the presence of a Fermi surface (FS)<sup>8,9,10,11,12</sup>.

In this work we continue to explore the field theoretical RG method. We calculate the renormalized form factors of the main physical instabilities of the two-dimensional HM up to two-loop order. We compare our results with other RG approaches in 2D<sup>9,10</sup>. Those results are summarized in the phase diagram which displays all leading and subleading instabilities in that dimension in coupling constant space. To reinforce our case we test our method in well known grounds and show it reproduces the analogous phase diagram in the one-dimensional case<sup>13</sup>. In 1D the coupling functions approach fixed point values producing susceptibilities which exhibit power-law behavior. This reflects the absence of spontaneous symmetry breaking and long-range order. We must keep this in

mind when analyzing the possible existing states in the phase diagrams of such low dimensional systems. Here in specifying such phase diagrams we need convenient to define appropriately symmetrized response functions with respect the spin projections of the corresponding particle-particle and particle-hole operators. In this way, we calculate the corresponding charge density wave (CDW), the spin density wave (SDW), the singlet superconductivity (SSC), and the triplet superconductivity (TSC) one-particle irreducible functions  $\chi_R^{(2;1)}$ 's which in turn define the respective susceptibilities.

In a 1D metal the FS reduces to two Fermi points ( $k_F$ ). In 2D, for non-interacting electrons, at half-filling the FS is a perfect square. If we go slightly away from half-filling, doping the system with holes, all corners get rounded and the area inside the FS is reduced from its square value. As a result in such conditions we may neglect the van Hove singularities as well as the Umklapp effects. In this 2D scenario a new symmetry arises with respect to the sign of momentum component along the FS. This will reflect itself in the RG equations for the renormalized form factors which we redefine as the charge density wave of s and d-types (CDW), the spin density wave of s and d-types (SDW), the singlet superconductivity of s and d-types (SSC) and, finally, the triplet superconductivity of s and d-types (TSC). All those symmetries are derived from the particle-particle and particle-hole operators which have a transform momentum  $q$ . Our results for the uniform spin and charge susceptibilities were presented in a separated publication<sup>14</sup>.

We showed in another work<sup>15</sup> that for such flat FS as soon as we add interactions to the 2D electron gas the flow to strong coupling destroys the Landau Fermi liquid regime. We demonstrated how the self-energy effects lead to the nullification of the quasiparticle weight directly affecting the RG equations for the renormalized coupling functions. In this work we discuss how those results also influence directly the response functions of the physical system. In particular we reveal that for the lightly doped 2D HM, all susceptibilities flow to fixed values. We argue that such a behavior suggests the exis-

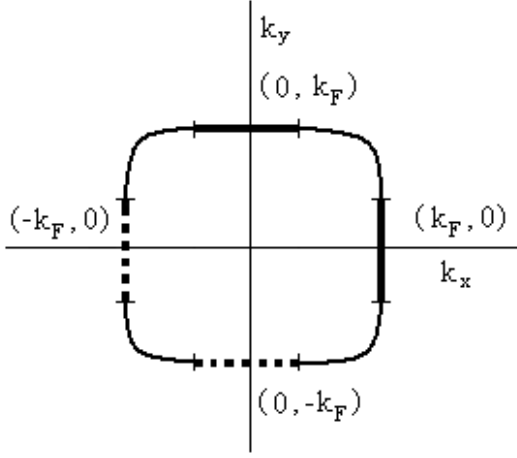


FIG. 1: The 2D Fermi surface with rounded corners. We divide it into four regions: two of the solid line type and two of the dashed line type. The perpendicular regions do not mix in our scheme.

tence of short-range correlations typical of a spin liquid phase. This is in agreement with our already mentioned uniform susceptibilities results<sup>14</sup>.

The presentation of our results begins with the derivation of the corresponding RG equations for the vertex functions and the associated susceptibilities within the field theory method. We discuss initially one-loop order results and show that they reproduce both the parquet and other fermionic RG schemes. Following this we present our new two-loop results. We show that the SDW and the d-wave superconductivity are indeed the leading instabilities in the physical system when the parallel component of the transfer momentum  $q_{\parallel}$  is equal to zero. Finally we conclude our work discussing the physical meaning of our results.

## II. THE MODEL

Firstly we consider a 2D lightly doped FS with no van Hove singularity as shown in Fig. 1. For convenience and to keep a closer contact with well-known works in one-dimensional physics<sup>13</sup>, we divide the FS into four regions. We restrict the momenta at the FS to the  $\alpha$  parts only. The contributions which originate in scattering processes associated with FS patches which are perpendicular to each other are irrelevant in the RG sense. For this reason we can select, for example, the patches centered at  $(0; k_F)$  and  $(0; -k_F)$  and simply neglect the other two. Following this we will restrict ourselves to the one-electron states labeled by the momenta  $p_{\parallel} = k_y$  and  $p_{\perp} = k_x$ . Accordingly the momenta parallel to the FS is restricted to the interval  $-\frac{\pi}{2} \leq p_{\parallel} \leq \frac{\pi}{2}$ , with  $\frac{\pi}{2}$  being essentially the size of the  $\alpha$  patches. In the same way the energy dispersion of the single-particle states is one-dimensional and given by  $\epsilon_{\alpha}(p) = v_F(p_{\parallel} - k_F)$  where  $v_F$  is the Fermi

velocity and the energy  $\epsilon$  is measured with respect to the chemical potential  $\mu$ . Notice that this dispersion relation depends only on the momenta perpendicular to the Fermi surface, where the label  $\alpha = \pm$  refers to the  $\alpha$  sectors at  $p_{\parallel} = \pm k_F$  respectively. In doing so we are only considering the  $\alpha$  parts whose nesting vectors are  $Q = (0; 2k_F)$ . We consider a fixed momentum cutoff which results in the interval  $k_F - \frac{\pi}{2} \leq p_{\parallel} \leq k_F + \frac{\pi}{2}$  for the perpendicular component in the vicinity of the FS. We neglect how the interactions renormalize the FS itself since it would be too complex to do otherwise at this stage. As a result, the momentum  $k_F$  will not be renormalized in our approach and will resume its noninteracting value. For the same reason, we will also neglect the Fermi velocity  $v_F$  momentum dependence along the FS.

Since we showed in detail all the necessary steps to do the renormalization in such a model up to two-loop order, from the start, we rewrite the renormalized Lagrangian  $L$  associated with the 2D Fermi surface entirely in terms of renormalized fields and couplings

$$L = \sum_{p; \alpha} \int \frac{d^4 p}{(2\pi)^4} \bar{\psi}_{R(\alpha)}(p) [i \partial_t - v_F(p_{\parallel} - k_F)] \psi_{R(\alpha)}(p) + \frac{1}{V} \sum_{p, q, k} \sum_{i=1}^4 \bar{\psi}_{R(+)}(p+q, k) [g_{2B} \psi_{R(-)}(k) \psi_{R(+)}(q) \psi_{R(+)}(p); \quad (2.1)$$

following the "g-ology" notation. Here the  $\psi_{R(\pm)}$  and  $\bar{\psi}_{R(\pm)}$  are, respectively, the creation and annihilation operators for particles located at the  $\pm$  patches. The couplings  $g_{1B}$  and  $g_{2B}$  stand for bare backscattering and forward scattering respectively.

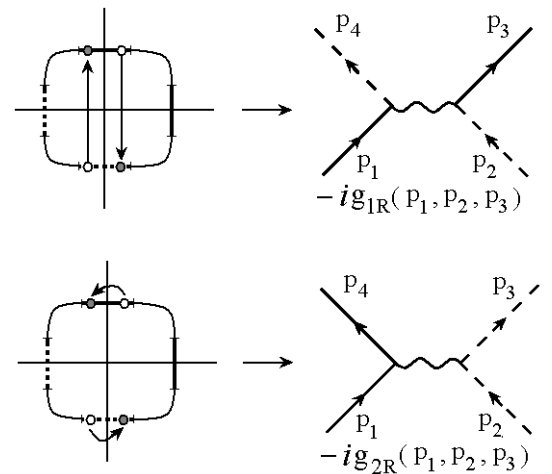


FIG. 2: The interaction processes in the model and the corresponding Feynman rules for the vertices. The  $g_{1R}$  and  $g_{2R}$  couplings stand for the renormalized backscattering and forward scattering respectively.

forward scattering couplings. From now on we will consider the thermodynamic limit ( $V \rightarrow \infty$ ) with all momenta summations becoming integrals such as  $\int \frac{d^2p}{(2\pi)^2}$ , with  $\sim = 1$ . Finally, the bare coupling functions are related to their renormalized associates by

$$g_{iB} = \frac{1}{Z} \sum_{i=1}^4 p_{ik} \left( g_{iR} + g_{iR} \right); \quad (2.2)$$

The diagrammatic representations of the corresponding renormalized forward and backscattering interactions are shown schematically in Fig 2. Here, we do not consider the Umklapp processes due to the fact that there is no superposition between our FS and the correspondingly Umklapp surface. In all Feynman diagrams, the non-interacting single-particle propagators  $G_{(+)}^{(0)}$  and  $G_{(-)}^{(0)}$  are represented by a solid and a dashed line respectively, following their association with the corresponding FS patches. They are given by

$$G_{(a)}^{(0)}(p) = \frac{1}{p_0 - \epsilon_a(p) + i} + \frac{1}{p_0 - \epsilon_a(p) - i} \quad (2.3)$$

Before we deal directly with the one-particle irreducible function  $\Gamma^{(2,1)}$ 's. In the next section we summarize the main results of the field theory for the quasiparticle weight and the coupling functions as well as the respective RG equations.

### III. RENORMALIZED COUPLING FUNCTIONS AND SELF-ENERGY UP TO TWO LOOPS

#### A. Self-energy and quasiparticle weight up to two-loops

In two-loop order another quantity plays an important role in the RG equations for the renormalized couplings: the quasiparticle weight  $Z$ . To calculate  $Z$  we must determine the renormalized self-energy  $\Sigma_R$ . Figure 3 displays the four important  $\Sigma_R$  diagrams for the determination of  $Z$  up to two-loop order. Those diagrams produce logarithmic singularities multiplied by the factor  $(p_0 - v_F(p_2 - j - k_F))$  which can only be canceled out by

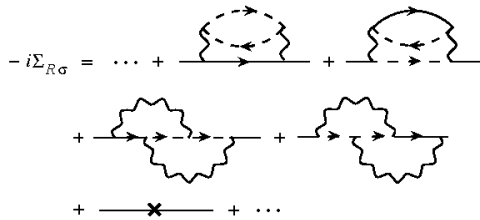


FIG. 3: The diagrams for the self-energy up to two-loops.

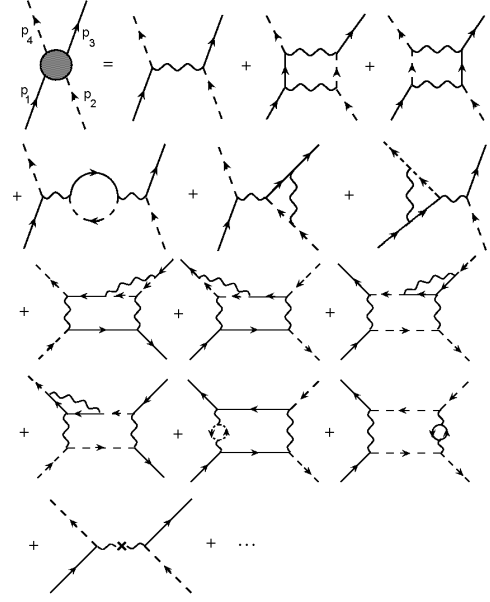


FIG. 4: The diagrams for the renormalized four-point vertex in the backscattering channel.

the corresponding counterterm diagram associated with the multiplicative fermion field factor  $Z$ . The use of an appropriate RG prescription for the one-particles Green's function at  $p_2 = k_F$  together with those contributions leads to the determination of  $Z$ . It then follows that the quasiparticle weight satisfies the RG equation

$$\mu \frac{\partial Z}{\partial \mu} = -Z \gamma; \quad (3.1)$$

where  $\gamma$  is the anomalous dimension. The full expression for  $\gamma$  is given in our Appendix A. The numerical estimation of  $Z$  follows our previous work. As we observe later the suppression of the quasiparticle weight as we strengthen the interactions changes dramatically the one-loop scenario.

#### B. Two-loop RG equations for the renormalized couplings

In Eq. (2.1) we wrote the renormalized Lagrangian which will automatically generate renormalized physical quantities in perturbation theory at any loop order. As a result, applying suitable Feynman rules one can arrive at the diagrams shown in the Fig. 4 and Fig. 5. The last diagrams in both sets are the counterterms which render the theory finite. In this way, we identify the renormalized one-particle irreducible  $\Gamma_{iR}^{(4)}$  ( $i = 1, 2$ ) such that, at the FS, the corresponding renormalized coupling functions  $g_{iR} p_{1k} p_{2k} p_{3k}$  are given by

$$\Gamma_{iR}^{(4)}(p_1; p_2; p_3) = i g_{iR}(p_1; p_2; p_3); \quad (3.2)$$

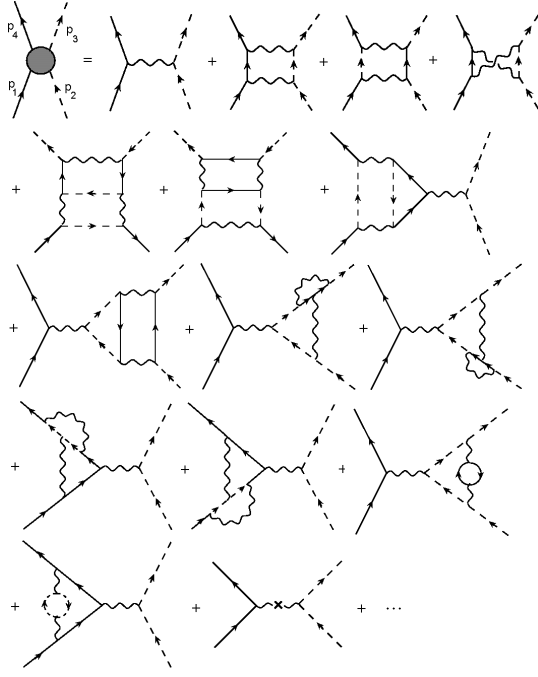


FIG. 5: The diagrams for the renormalized four-point vertex in the forward scattering channel.

Taking into account the associated  $Z$  factors for the external momenta and the RG conditions  $dg_{iB}/d\ell = 0$  for the bare coupling functions the RG equations for the coupling functions follow immediately

$$\ell \frac{dg_{iR}(p_{1k}; p_{2k}; p_{3k})}{d\ell} = \frac{1}{2} \sum_{j=1}^4 p_{jk} g_{iR}(p_{1k}; p_{2k}; p_{3k}) - \ell \frac{\partial g_{iR}(p_{1k}; p_{2k}; p_{3k})}{\partial \ell} : (3.3)$$

where  $i = 1; 2$ . We make use of the numerical estimates of those RG equations in the calculations presented in this work. Having said that we are now set to implement the RG strategy to calculate the renormalized form factors which are indeed the linear response functions of the

system for the at FS in 2D.

#### IV. RESPONSE FUNCTIONS

Following the RG strategy to study the pairing and density wave instabilities of the system let us add initially to the renormalized Lagrangian of the system two infinitesimal external fields  $h_{SC}$  (for the pairing term) and  $h_{DW}$  (for the density wave) which act essentially as source fields for the generation of particle-particle and particle-hole pairs. That is, we include in our renormalized Lagrangian the contributions

$$L_{ext} = \frac{1}{V} \sum_{k,q} Z^{1/2}(k_k) Z^{1/2}(q_k - k_k) h_{SC}(q) T_{SC}^B(k; q) + \sum_{R(+)} \langle k \rangle \sum_{R(-)} \langle q - k \rangle + Z^{1/2}(k_k) Z^{1/2}(k_k - q_k) h_{DW}(q) T_{DW}^B(k; q) + \sum_{R(+)} \langle k \rangle \sum_{R(-)} \langle k - q \rangle + H.c. : (4.1)$$

where  $T_i^B(k; q)$  ( $i = SC; DW$ ) is a bare form factor which is determined in such a way to incorporate the symmetry it is associated with. Notice that in this model the external fields are made spin dependent since this is important for the definition of some symmetries which we will refer next. As we have done in section II we will consider again the thermodynamic limit with all momenta summations becoming integrals. By means of the added Lagrangian  $L_{ext}$  we are now able to generate the one-particle irreducible functions associated with the composite pairing and the composite particle-hole operators. Since we are interested in the response functions for the density wave and superconductor channels we need to define the associated three points generalized Green's functions namely  $G_{DW}^{R(2;1)}$  and  $G_{SC}^{R(2;1)}$ . In doing this we get back the corresponding  $G_{DW}^{R(2;1)}$  and  $G_{SC}^{R(2;1)}$  by cutting out the external legs of the corresponding  $G_i^{R(2;1)}$ 's. The  $G_i^{R(2;1)}$ 's are given by

$$G_{DW}^{R(2;1)}(p; q) = i \frac{\langle p \rangle \langle q \rangle}{h_{DW}(q)} \exp \left[ i \int_{q_0 p_0}^Z L_{ext}(h_{DW}; h_{SC}) \right]_{h_{DW}=0} \quad (4.2)$$

and

$$G_{SC}^{R(2;1)}(p; q) = i \frac{\langle p \rangle \langle q \rangle}{h_{SC}(q)} \exp \left[ i \int_{q_0 p_0}^Z L_{ext}(h_{DW}; h_{SC}) \right]_{h_{SC}=0} \quad (4.3)$$

where  $\langle \dots \rangle$  stands for  $\frac{1}{V} \int d^3x \exp[iS] \dots$  with  $S$  being the classical action associated with the

renormalized Lagrangian given by Eq. (2.1).

Following conventional Feynman rules we display the diagrams in Fig. 6 for the density wave and superconductor channels up to one-loop order respectively.

Notice that the  $^{(2;1)}_R$  counterterm diagrams cancel exactly all the corresponding higher order diagrams which scale as  $(\ln(\Lambda))^n$  with  $n \geq 2$ . Moreover, there are no other linearly log divergent diagrams in  $^{(2;1)}_R$ . Consequently, in our scheme the resulting higher loop effects in higher order contributions for  $^{(2;1)}_R$  are produced by the  $Z$  factors in our RG equations. Hence, if we consider the external Lagrangian (4.1) we can rewrite the bare form factors such that

$$T_{DW}^B(p; q) = Z^{1=2}(p_k; !) Z^{1=2}(p_k - q_k; !)$$

$$Z_{DW}^{1=2}(p_k; q_k; !) T_{DW}^R(p; q) \quad (4.4a)$$

$$T_{SC}^B(p; q) = Z^{1=2}(p_k; !) Z^{1=2}(q_k - p_k; !)$$

$$Z_{SC}^{1=2}(p_k; q_k; !) T_{SC}^R(p; q) \quad (4.4b)$$

or, equivalently

$$T_{DW}^B(p; q) = Z_h^{1=2}(p_k; !) Z_h^{1=2}(p_k - q_k; !)$$

$$T_{DW}^R(p; q) + T_{DW}^R(p; q) \quad (4.5a)$$

$$T_{SC}^B(p; q) = Z_h^{1=2}(p_k; !) Z_h^{1=2}(q_k - p_k; !)$$

$$T_{SC}^R(p; q) + T_{SC}^R(p; q) \quad (4.5b)$$

The counterterm ( $T_{DW(SC)}^R$ ) guarantees the cancellation of the divergent vertex functions diagrams in one-loop order. This renders the theory finite at the FS.

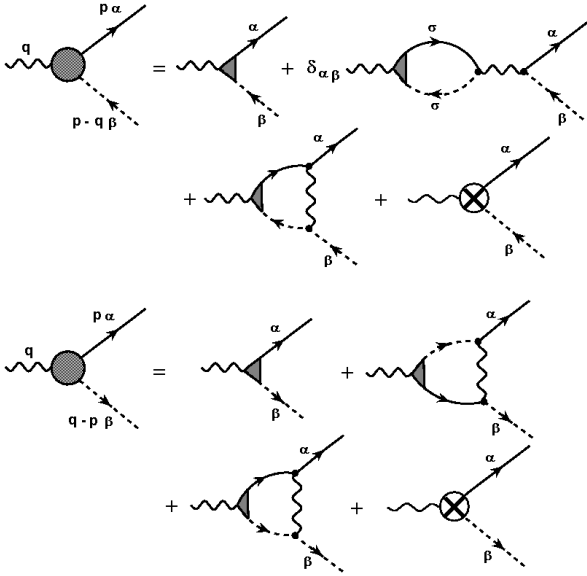


FIG. 6: The Feynman diagram up to one-loop order for the renormalized  $T_{DW}^R$  in the density wave channel and the renormalized  $T_{SC}^R$  in the superconductor channel.

Notice that the renormalized form factors depend on the momenta  $p$  and  $q$ . Now, we are ready to set up the prescriptions for the renormalized one-particle irreducible Green's functions  $^{(2;1)}_{Ri}$ 's, in terms of experimentally observable physical quantities

$$T_{DW}^{R(2;1)}(p_k; p_0 = !; p_? = k_F; q_k; p_? = 2k_F) =$$

$$iT_{DW}^R(p_k; q_k) \quad (4.6a)$$

$$T_{SC}^{R(2;1)}(p_k; p_0 = !; p_? = k_F; q_k; p_? = 0) =$$

$$iT_{SC}^R(p_k; q_k): \quad (4.6b)$$

As we already mentioned all renormalized quantities are RG energy scale dependent. However, to avoid overloading notations we omit this dependence from now on except when it is strictly necessary to do so. In this way, considering the diagrams shown in Fig 6 and making use of the RG conditions stated in Eqs. (4.6a) and (4.6b) we arrive at

$$T_{DW}^R = \frac{1}{4^{2V_F}} \int_{D_1} dk_k \sum_{\alpha} g_{1R}(k_k; p_k - q_k; p_k)$$

$$T_{DW}^R(k_k; q_k) - g_{2R}(k_k; p_k - q_k; p_k)$$

$$T_{DW}^R(k_k; q_k) \ln \frac{\Lambda}{\mu} \quad (4.7a)$$

$$T_{SC}^R = \frac{1}{4^{2V_F}} \int_{D_2} dk_k g_{2R}(k_k; q_k - k_k; q_k - p_k)$$

$$g_{1R}(k_k; q_k - k_k; p_k) T_{SC}^R(k_k; q_k) \ln \frac{\Lambda}{\mu} \quad (4.7b)$$

Consistently with the renormalized density wave and pairing form factors  $T_{DW}^R$  and  $T_{SC}^R$  we can now do the symmetrization with respect to the spin components to define

$$T_{CDW}^R(p_k; q_k) = T_{DW}^{R'''}(p_k; q_k) + T_{DW}^{R\#\#}(p_k; q_k) \quad (4.8a)$$

$$T_{SDW}^R(p_k; q_k) = T_{DW}^{R'''}(p_k; q_k) - T_{DW}^{R\#\#}(p_k; q_k) \quad (4.8b)$$

$$T_{SSC}^R(p_k; q_k) = T_{SC}^{R''\#}(p_k; q_k) - T_{SC}^{R\#\#}(p_k; q_k) \quad (4.8c)$$

$$T_{TSC}^R(p_k; q_k) = T_{SC}^{R''\#}(p_k; q_k) + T_{SC}^{R\#\#}(p_k; q_k) \quad (4.8d)$$

where (CDW) relates to charge density wave, (SDW) to spin density wave, (SSC) to singlet superconductivity and (TSC) to triplet superconductivity respectively. Now, we can differentiate the equations (4.5a) and (4.5b) with respect to  $\Lambda$  to get

$$\begin{aligned} \frac{d}{d!} T_{DW}^B &= \frac{d}{d!} Z^{1=2} (p_k; ! ) Z^{1=2} (p_k \quad q_k; ! ) \\ &T_{DW}^R (p_k; q_k) + T_{DW}^R (p_k; q_k) \end{aligned} \quad (4.9a)$$

$$\begin{aligned} \frac{d}{d!} T_{SC}^B &= \frac{d}{d!} Z^{1=2} (p_k; ! ) Z^{1=2} (q_k \quad p_k; ! ) \\ &T_{SC}^R (p_k; q_k) + T_{SC}^R (p_k; q_k) \end{aligned} \quad (4.9b)$$

Taking into account the fact that the bare quantities do not know anything about the RG scale we can arrive at

$$\begin{aligned} \frac{d}{d!} T_{DW}^R (p_k; q_k) &= \frac{d}{d!} T_{DW}^R (p_k; q_k) \\ &+ \frac{1}{2} T_{DW}^R (p_k; q_k) (p_k; ! ) + (p_k \quad q_k; ! ) \end{aligned} \quad (4.10a)$$

$$\begin{aligned} \frac{d}{d!} T_{SC}^R (p_k; q_k) &= \frac{d}{d!} T_{SC}^R (p_k; q_k) \\ &+ \frac{1}{2} T_{SC}^R (p_k; q_k) (p_k; ! ) + (q_k \quad p_k; ! ) \end{aligned} \quad (4.10b)$$

where  $\epsilon$  is the anomalous dimension. Since we have already defined the symmetrized renormalized form factors with respect to spin projection, we are now able to write down their corresponding RG equations

$$\begin{aligned} \frac{d}{d!} T_b^R (p_k; q_k) &= \frac{d}{d!} T_b^R (p_k; q_k) + \frac{1}{2} T_b^R (p_k; q_k) \\ &(p_k; ! ) + (p_k \quad q_k; ! ) \end{aligned} \quad (4.11a)$$

$$\begin{aligned} \frac{d}{d!} T_c^R (p_k; q_k) &= \frac{d}{d!} T_c^R (p_k; q_k) + \frac{1}{2} T_c^R (p_k; q_k) \\ &(p_k; ! ) + (q_k \quad p_k; ! ) \end{aligned} \quad (4.11b)$$

where  $b = CDW; SDW$  and  $c = SSC; TSC$ . The full expressions for the symmetrized counterterms  $T_i^R$ 's for the anomalous dimension is given in Appendix A. Due to the particular shape of our  $\epsilon$  at FS, the renormalized couplings must be symmetrical with respect to the exchange of upper(right) and lower(left) particles and the change of sign of the external  $p_{ik}$ 's. It then follows that

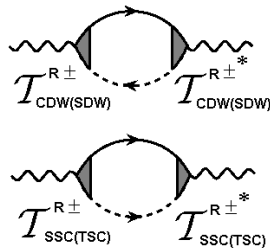


FIG. 7: The respective susceptibilities generated from the renormalized form factors  $T_{CDW(SDW)}^R$  and  $T_{SSC(TSC)}^R$ .

$$\begin{aligned} g_{iR} (p_{1k}; p_{2k}; p_{3k}; p_{4k}) &= g_{iR} (p_{1k}; p_{2k}; p_{3k}; p_{4k}) \\ g_{iR} (p_{1k}; p_{2k}; p_{3k}; p_{4k}) &= g_{iR} (p_{2k}; p_{1k}; p_{4k}; p_{3k}) \\ g_{iR} (p_{1k}; p_{2k}; p_{3k}; p_{4k}) &= g_{iR} (p_{4k}; p_{3k}; p_{2k}; p_{1k}) \end{aligned} \quad (4.12)$$

These conditions need to be satisfied by the RG equations in order for them to produce the correct numerical results when we approach the FS. These symmetries are satisfied by the RG equations (4.11a) and (4.11b) which are symmetrical with respect to the sign reversal of  $p_k$  for a fixed  $q_k$ . Following this we can therefore define two irreducible representations of this symmetry which never mix with each other

$$T_b^R (p_k; q_k) = T_b^R (p_k; q_k) \quad T_b^R (p_k; q_k) \quad (4.13a)$$

$$T_c^R (p_k; q_k) = T_c^R (p_k; q_k) \quad T_c^R (p_k; q_k) \quad (4.13b)$$

where again  $b = CDW; SDW$  and  $c = SSC; TSC$ . The  $(+)$  sign is associated with the s-wave symmetry whereas the  $(-)$  sign is associated with the d-wave symmetry instead. Now, considering the symmetries of the couplings (4.12) and the new symmetrized form factors (4.13a) and (4.13b) we can write the RG equations (4.11a) and (4.11b) in the following way

$$\begin{aligned} \frac{d}{d!} T_b^R (p_k; q_k) &= \frac{d}{d!} T_b^R (p_k; q_k) + \frac{1}{2} T_b^R (p_k; q_k) \\ &(p_k; ! ) + (p_k \quad q_k; ! ) \end{aligned} \quad (4.14a)$$

$$\begin{aligned} \frac{d}{d!} T_c^R (p_k; q_k) &= \frac{d}{d!} T_c^R (p_k; q_k) + \frac{1}{2} T_c^R (p_k; q_k) \\ &(p_k; ! ) + (q_k \quad p_k; ! ) \end{aligned} \quad (4.14b)$$

where the expressions for  $T_{CDW}^R$ ,  $T_{SDW}^R$ ,  $T_{SSC}^R$ ,  $T_{TSC}^R$  can be found in the Appendix B. The plus sign in the DW's is associated with the charge and spin density waves. However, the minus sign symmetry of the parallel momentum along the FS in the DW's yield circular charge (spin) currents flowing around the square lattice with alternating directions. In this way we associate this symmetry of the DW's with the charge and spin current waves also known as flux phases. Once the renormalized  $T_{CDW(SDW)}^R$  and  $T_{SSC(TSC)}^R$  are found we can define the related susceptibilities following the diagrammatic scheme shown in Fig. 7. As one can see there is a IR divergent bubble in each channel. As a result we get

$$\begin{aligned} T_b^R (q_k; ! ) &= \frac{1}{4 \cdot 2 v_F} \ln \frac{1}{\Lambda} \int_{D_3} dp_k T_b^R (p_k; q_k) \\ &T_b^R (p_k; q_k) \end{aligned} \quad (4.15a)$$

$$\begin{aligned} T_c^R (q_k; ! ) &= \frac{1}{4 \cdot 2 v_F} \ln \frac{1}{\Lambda} \int_{D_4} dp_k T_c^R (p_k; q_k) \\ &T_c^R (p_k; q_k) \end{aligned} \quad (4.15b)$$

where  $D_3$  and  $D_4$  are the intervals determined in the Appendix B and b and c refer to the symmetries mentioned before. Notice that if we don't go beyond one-loop order all RG equations for the susceptibilities approach the strong coupling regime. As a result all susceptibilities diverge in the IR limit at that order of perturbation theory. In two-loop order we show that only one susceptibility at a time remains divergent and all the others approach fixed plateau values instead. Having said that we also call attention to the fact that in two-loops the leading susceptibility approaches the strong coupling regime in a much slower rate than the one found in one-loop order. This might mean that the IR divergence may disappear altogether in the presence of higher order corrections and as a result one should not expect true long-range order if all this is taken into account. We discuss this further later on. From Eqs. (4.15a) and (4.15b) we arrive immediately at the RG equations for the various susceptibilities

$$\frac{d}{d\ell} \chi_b^R(q_k; \ell) = \frac{1}{4^2 v_F} \int_{D_3} dp_k T_b^R(p_k; q_k) \quad (4.16a)$$

$$\frac{d}{d\ell} \chi_c^R(q_k; \ell) = \frac{1}{4^2 v_F} \int_{D_4} dp_k T_c^R(p_k; q_k) \quad (4.16b)$$

These expressions are written in general form. However, since we are just considering  $g_{1R}$  and  $g_{2R}$  couplings it turns out that  $T_{b;c}^R = T_{b;c}^R$ .

## V. RESULTS

In order to solve all those RG equations we have to resort to numerical methods since we want to estimate how the order parameters change as we vary the scale  $\ell$  to take the physical system towards the FS. As we have

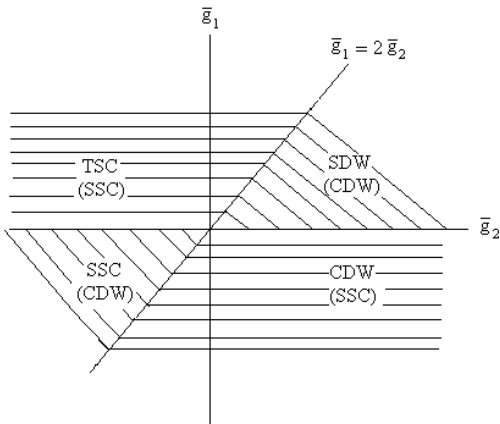


FIG. 8: Phase diagram for the susceptibilities in one-dimension up to two-loops.

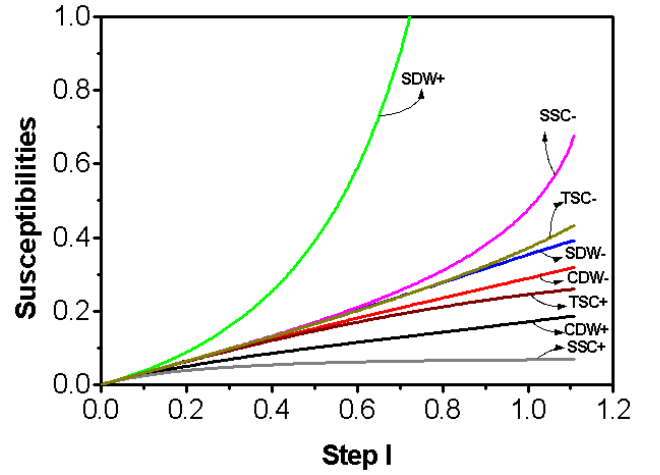


FIG. 9: Susceptibilities  $\chi_{a,b}^R(q_k = 0; \ell)$  against step  $\ell$  for one-loop approach with  $\bar{g}_{1R} = \bar{g}_{2R} = 10$  as initial conditions for the couplings. The SDW  $\pm$  type diverges for  $\ell > 1.2$ .

done in an earlier work we discretize the FS continuum replacing the interval  $[-6, 6]$  by a discrete set of 33 points. For convenience, we use  $\ell = \exp(-l)$ , where  $\ell = 2k_F$  with  $l$  being our RG step. We choose  $v_F = 1$ . In view of our choice of points for the FS, we are only allowed to go up to  $\ell = 2.8$  in the RG flow to avoid the distance  $\ell$  to the FS being smaller than the distance between neighboring points since the discretization procedure no longer applies in this case.

The RG equations for all couplings considered here were reproduced in section III. As a result all RG equations (3.1), (3.3), (4.11a) and (4.11b) and (4.16a) and (4.16b) have to be solved simultaneously. Hence, the numerical estimates become much more involved.

To improve the understanding of our results we also

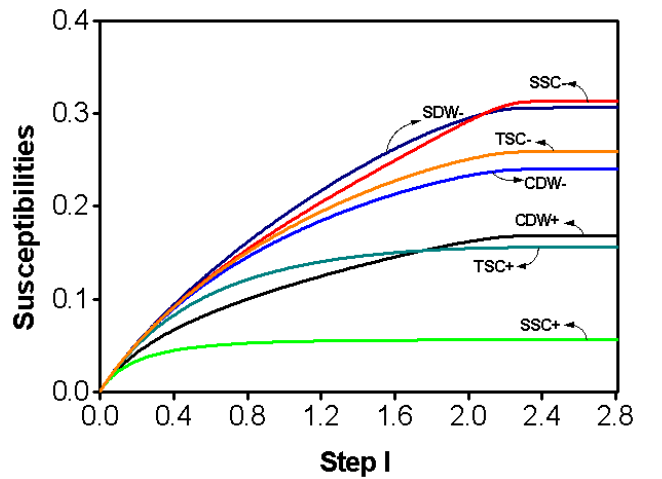


FIG. 10: Susceptibilities  $\chi_{a,b}^R(q_k = 0; \ell)$  against step  $\ell$  for two-loop approach with  $\bar{g}_{1R} = \bar{g}_{2R} = 10$  as initial conditions for the couplings.

consider the one-dimensional limits of all our RG equations. We reproduce all those one-dimensional RG equations in our appendix C. Following the same scheme used for  $D = 2$  all one-dimensional RG equations are solved numerically in a self-consistent manner. Notice that as expected the equation  $!d(g_{1R} - 2g_{2R})=d! = 0$  is trivially satisfied. In Fig. 8 we display the one-dimensional phase diagram in coupling space. This phase diagram is constructed in the usual way taking into account the two dominant susceptibilities that diverge for a given initial values of the renormalized couplings  $g_{1R}$  and  $g_{2R}$ . We do that because there are always two divergent susceptibilities in all region of the phase space. Our numerical estimates are in good agreement with Solyom's earlier RG results<sup>13</sup>. However, we noticed that those divergences take place only when the RG step is too large or, equivalently,  $!$  is very small. This effect is amplified as we move from one-loop to two-loops. As a result despite the fact that there might be strong collective fluctuations in such a system we cannot say that they are of long range type since when we consider higher orders in our perturbation theory the divergences only take place in even larger RG steps. This situation will reflect itself more emphatically in the two-dimensional case as we will see next.

Now, we move on to our original RG equations in two-dimensions. The choice of the initial conditions at  $l = 0$  in the RG equations are, in principle, arbitrary. However, as we have done before, we set the couplings equal to each other to mimic the Hubbard on-site repulsive interaction parameter  $U$  in our RG scheme. Namely  $\bar{g}_{1R} = \bar{g}_{2R} = 10$ , where  $\bar{g}_{iR} = g_{iR} / v_F$ . In another paper we give more details about this connection with the Hubbard model<sup>14</sup>.

In order to reproduce some symmetries of the order parameters with respect to FS we choose the following

initial conditions ( $l = 0$ )

$$\begin{aligned} T_{CDW}^{R+}(p_k; q_k) &= T_{SDW}^{R+}(p_k; q_k) = T_{SSC}^{R+}(p_k; q_k) = \\ &T_{TSC}^{R+}(p_k; q_k) = 1 \end{aligned} \quad (5.1a)$$

$$\begin{aligned} T_{CDW}^R(p_k; q_k) &= T_{SDW}^R(p_k; q_k) = T_{SSC}^R(p_k; q_k) = \\ &T_{TSC}^R(p_k; q_k) = \frac{p_k}{2} \sin \frac{p_k}{2} \end{aligned} \quad (5.1b)$$

Notice that despite the fact that the initial values of the form factor are either unity or a function of  $p_k$  the  $q_k$  dependence is generated naturally by the renormalization process. The choice made for the symmetrized (+) vertices is motivated by their independence with respect to the change of sign of  $p_k$ . In contrast with the antisymmetric vertices our choice is oriented by our need to reproduce the symmetries of the flux phases and the  $d_{x^2-y^2}$  superconductivity with respect to the FS. Furthermore, we take all susceptibilities equal to zero at  $l = 0$ , that is,  $\chi_i(q_k; l = 0) = 0$  ( $i = CDW; SDW; SSC; TSC$ ).

To arrive at the final results we do a simultaneous calculation of the renormalized form factors and the corresponding susceptibilities together with the flow equations for the coupling functions  $g_{1R}$  and  $g_{2R}$ . It emerges from our numerical estimates that the SDW of symmetry type  $s$  produces the dominant susceptibility when the transfer momentum is equal to the nesting vector ( $q = Q$ ). To make the comparison of our results with previous estimates found in the literature we display our computations in two steps. Initially we show the one-loop order results since they can be compared directly with calculations presented by other groups. Next, we move on to display our two-loop calculations. Following that we discuss the most interesting results and the difference between our estimates in one-loop and two-loops.

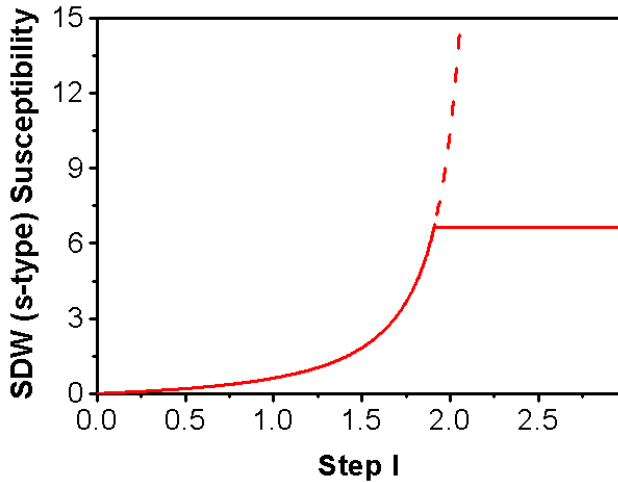


FIG. 11: SDW + susceptibility  $\chi_{SDW}^+(q_k; l)$  with  $\bar{g}_{1R} = \bar{g}_{2R} = 10$  as initial conditions for the couplings. The SDW  $s$ -type diverges for  $l = 2.15$ . Dashed line refers to perfect nesting of the FS. Solid line refers to the RG step  $l = l_{cut-off}$  considering a "corrugation" in the FS.

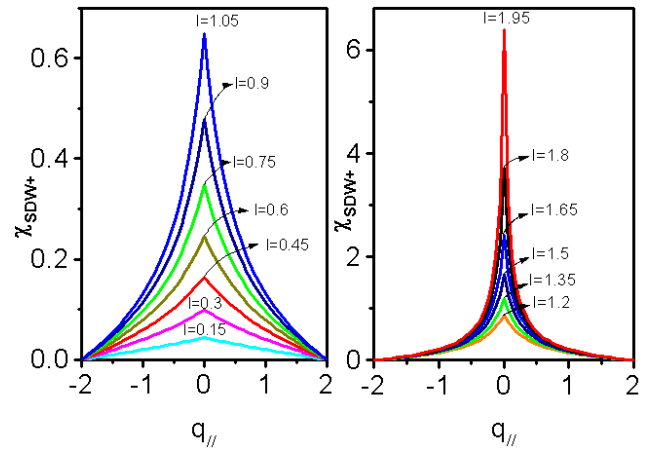


FIG. 12: SDW + susceptibility  $\chi_{SDW}^+(q_k; l)$  against  $q_k$  for several RG steps with  $\bar{g}_{1R} = \bar{g}_{2R} = 10$  as initial conditions for the couplings.



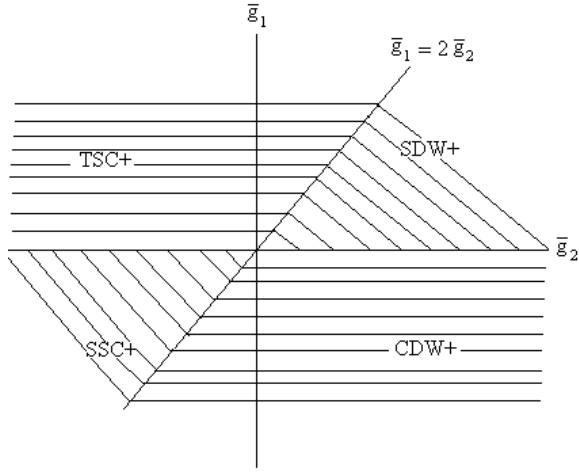


FIG. 13: The leading susceptibilities for several initial values of coupling functions.

#### A. One-loop RG approach

The one-loop results for all susceptibilities are displayed in Fig. 9. As can be seen all susceptibilities diverge but the leading one is the SDW + symmetry in the repulsive HM like regime. According to this, we should expect an insulating spin density wave state and no sign of even nonconventional metallic behavior in the physical system. It is interesting to observe that the second most pronounced renormalized susceptibility corresponds to a  $d_{x^2-y^2}$  superconductivity symmetry.

Our result is consistent with other approaches based on one-loop fermionic functional RG<sup>9</sup> and the so-called parquet method<sup>11</sup>. In all those approaches, the feedback of the quasiparticle weight  $Z$  is not taken into account. The fact that  $Z \neq 0$  produces drastic changes in the flow of all RG equations in two-loops as we will see next.

#### B. The full two-loop approach

In this case, we solve the Eqs. (4.11a) and (4.11b) and Eqs. (4.16a) and (4.16b) simultaneously with the RG equations for the renormalized couplings using the same initial conditions given by Eqs. (5.1a) and (5.1b), namely,  $(q_k; l=0) = 0$  and  $\bar{g}_{1R} = \bar{g}_{2R} = 10$  respectively.

The results obtained for all susceptibilities excluding the SDW + are shown in Fig. 10. As one can see the effect of  $Z$  in the RG equations changes drastically the one-loop scenario. Notice that the plateau values appear at  $l = 2.2$  for almost all susceptibilities, that is, when the strong renormalization of the coupling functions takes place. In contrast with the picture described for the coupling functions at the same two-loop order, these plateaus are real fixed points since their values are not sensitive to our FS discretization procedure. Thus, we can infer from this, that with the exception of the SDW + symmetry, all existing order parameters appear

as short range correlations. However, for this HM like scenario, the SDW + symmetry manifests itself in a completely different manner and to illustrate this we plotted the SDW + susceptibility as a function of the parallel transfer momentum ( $q_k$ ) in Fig. 12.

As  $q_k$  approaches zero the SDW + susceptibility increases drastically as a function of the RG step  $l$ . In contrast for any other value for the parallel transfer momentum ( $q_k \neq 0$ ) the RG equation for  $\chi_{SDW}^{R+}$  flows to a given fixed value. Does this mean that we can assign to the SDW + divergence at  $q_k = 0$  a long-range type correlation? As we emphasized earlier the effect of the quasiparticle weight in two-loop approach the SDW + divergence becomes predominant for larger values of the renormalization step  $l$ . This is a strong evidence that even this divergence might not be what it seems. In fact, we expect that if we were to consider higher order contributions in perturbation theory this divergence would occur for even larger  $l$  values. In order to interpret correctly the meaning of this divergent susceptibility we have to keep in mind the limitations of our RG analysis. From the start we said that we were dealing with a two-dimensional FS with rounded corners. This FS represents a doped electron system slightly away from half-filling. As a result there exists a non-zero chemical potential which is an indirect measure of that doping regime. It introduces a new scale into the problem. At RG scales  $l \gg l_c$  we can safely treat the FS as being made of perfectly flat patches with rounded corners. As  $l_c$  is lowered (i.e. as we increase the number of RG steps) our RG resolution of FS must be corrected to include its "corrugation" effects. To take this resolution effect approximately into account we follow Zheleznyak et al<sup>11</sup> in establishing a cutoff  $l_c$  beyond which we are no longer able to be sure about the perfect flatness of our FS.

We take  $l_c$  such that  $l_c = \ln(\text{cutoff} = j) = 1.95$  since  $\chi_{SDW}^{R+}$  only diverges for  $l = 2.15$ . This means that for  $l = l_c$  the SDW s-type will now reach a plateau value before this divergence takes place. We display this new  $\chi_{SDW}^{R+}$  in Figure 11. This excludes the existence of long-range order in such a lightly doped Hubbard model like regime.

In Figure 13 we display a phase diagram with the leading susceptibilities for several initial conditions of the coupling functions. In our calculations we notice that when we set initial values for the couplings nearby each axis the symmetry associated with the next phase becomes more pronounced. As an example, if we are in the SDW + phase and we choose initial conditions nearby the straight line  $\bar{g}_1 = 2\bar{g}_2$  we obtain as a result an increase in the TSC+ susceptibility and so on. Moreover, we can emphasize that this phase diagram is quite different from that in one-dimension. The latter shows the possible ground states inferred from the renormalized form factors which in turn are a mixture of two states while in two-dimensions there is only one pronounced susceptibility at a time which we associate with a strong collective

oscillation. This shows how much the one-dimensional scenario can change as one goes from one to two dimensions.

## VI. CONCLUSION

In this paper we have performed a full two-loop theoretical RG calculation for the symmetries CDW<sup>-</sup>;SDW<sup>-</sup>;SSC and TSC in the presence of a square two dimensional FS with rounded corners. We neglected Umklapp effects at this stage since we are not at half-filling. To render the theory finite we applied the RG field theory by adding appropriate counterterms order by order in perturbation theory.

Due to the particular shape of our FS we can reproduce some symmetries by just choosing appropriate initial conditions for the renormalized form factors. The general expectation is that the resulting physical state has several competing instabilities such as the flux phases (CDW<sup>-</sup> and SDW<sup>-</sup>), the singlet  $d_{x^2-y^2}$  superconductivity (SSC<sup>-</sup>), the d-type triplet superconductivity (TSC<sup>-</sup>), the singlet and triplet superconductivity of s-type (SSC<sup>+</sup> and TSC<sup>+</sup>) and finally the spin density wave (SDW<sup>+</sup>) and charge density wave (CDW<sup>+</sup>). At one-loop order all those symmetries diverge and the leading divergence is SDW<sup>+</sup> suggesting that there is a long-range type correlation.

In two-loop order for the repulsive HM like initial conditions we obtained that all susceptibilities go to stable fixed points except the SDW<sup>+</sup> symmetry that continues to diverge in this case. In order to interpret correctly the meaning of this divergent susceptibility we call attention to the fact that the divergence in two-loop order takes place for larger values of the RG step  $l$  in comparison with what is obtained in one-loop order. It is therefore reasonable to expect that in higher orders the divergence takes place for even higher values of  $l$ . This happens due to the limitation of the RG analysis.

In this model we assumed that the FS is completely flat and, as a result, perfectly nested. However, in real situations, this naive assumption breaks down since most FS's are expected to exhibit a finite curvature at some critical scale  $k_c$  as one approaches the low-energy limit. In such a condition the nesting is destroyed. If this happens, the RG flow of the susceptibility associated with the SDW<sup>+</sup> order parameter will become interrupted due to the fact that this quantity strongly relies on the nesting properties of our FS model. Consequently, this result asserts that there should be only short-range order in the system in agreement with the general expectation that strong quantum fluctuations should be a dominant feature in such low dimensional systems.

We sketched the phase diagram for different renormalized coupling constants initial conditions in two dimensions. There is only one pronounced susceptibility at a time which we associate with a dominant collective oscillation. In order to test our method in well known grounds we solved all RG equations for one-dimensional

case. We reproduce correctly the phase diagram displayed earlier by Solyom<sup>13</sup> together with the possible ground states of the system inferred by renormalized form factors.

To have a better idea about the nature of the dominant instability we have to calculate the corresponding uniform susceptibilities which are calculated taking the transfer momentum equal to zero ( $q = (0;0)$ ). This has been done in a recent paper for the particular case of the repulsive HM like initial conditions. We obtained in case that the charge compressibility flows to zero, that is,  $\partial n / \partial \mu \rightarrow 0$  and, hence, we could indeed consider that the SDW<sup>+</sup> divergence would lead to a symmetry breaking contradicting all arguments presented previously. However, another quantity flows to zero as well. When we calculate the uniform spin susceptibility we find the opening of a spin gap as  $\chi_{\text{spin}}^{\text{uniform}} \rightarrow 0$ . Hence, it is our belief that the quantum regime associated with such a state is characteristic of an insulating spin liquid. This conclusion is in agreement with the results presented in this work.

This work was partially supported by the Conselho Nacional de Desenvolvimento Científico e Tecnológico (CNPq).

## APPENDIX A

In this appendix, we write down the explicit form of the  $T_i^R$ 's ( $i = \text{CDW}^-; \text{SDW}^-; \text{SSC}; \text{TSC}$ ) and  $\chi_i$ 's which are taken into account in the Eqs. (4.11a), (4.11b), (4.14a) and (4.14b). We also give the several intervals of integration that are considered throughout this work. They are following

$$D_1 = \begin{matrix} 8 \\ > \\ & 6 k_k 6 \\ & 6 p_k 6 \\ & 2 \quad 6 q_k 6 \quad 2 \\ & 6 p_k \quad q_k 6 \end{matrix} ;$$

$$D_2 = \begin{matrix} 8 \\ \wedge \\ & 6 k_k 6 \\ & 6 p_k 6 \\ & 2 \quad 6 q_k 6 \quad 2 \\ \wedge \\ & 6 q_k \quad k_k 6 \\ & 6 q_k \quad p_k 6 \end{matrix} ;$$

$$D_3 = \begin{matrix} 8 \\ < \\ & 6 p_k 6 \\ & 2 \quad 6 q_k 6 \quad 2 \\ : \\ & 6 p_k \quad q_k 6 \end{matrix} ;$$

$$D_4 = \begin{matrix} 8 \\ < \\ & 6 p_k 6 \\ & 2 \quad 6 q_k 6 \quad 2 \\ : \\ & 6 q_k \quad p_k 6 \end{matrix} ;$$

$$D_5 = \begin{array}{c} 8 \\ \sim \\ \sim \\ \sim \end{array} \begin{array}{c} 6 k_k 6 ; \\ 6 p_k 6 ; \\ 6 q_{1k} 6 ; \\ 6 k_k + p_k + q_{1k} 6 : \end{array}$$

$$D_6 = \begin{array}{c} 8 \\ \sim \\ \sim \\ \sim \end{array} \begin{array}{c} 6 k_k 6 ; \\ 6 p_k 6 ; \\ 2 6 q_k 6 2 ; \\ 6 q_{1k} 6 ; \\ 6 k_k + p_k q_k + q_{1k} 6 : \end{array}$$

$$D_7 = \begin{array}{c} 8 \\ \sim \\ \sim \\ \sim \end{array} \begin{array}{c} 6 k_k 6 ; \\ 2 6 q_k 6 2 ; \\ 6 p_k 6 ; \\ 6 q_{1k} 6 ; \\ 6 k_k + q_k p_k + q_{1k} 6 : \end{array}$$

We begin with the expressions for the  $T_i^R$ 's associated with  $(2;1)$ 's. We get

$$T_{CDW}^R(p_k; q_k) = \frac{1}{4^{2V_F}} \ln \frac{1}{!} \int_{D_1} dk_k 2g_{1R} k_k; p_k q_k; p_k g_{2R} k_k; p_k q_k; k_k q_k T_{CDW}^R(k_k; q_k); \quad (A1)$$

$$T_{SDW}^R(p_k; q_k) = \frac{1}{4^{2V_F}} \ln \frac{1}{!} \int_{D_1} dk_k g_{2R} k_k; p_k q_k; k_k q_k T_{SDW}^R(k_k; q_k); \quad (A2)$$

$$T_{SSC}^R(p_k; q_k) = \frac{1}{4^{2V_F}} \ln \frac{1}{!} \int_{D_2} dk_k g_{1R} k_k; k_k + q_k; p_k + g_{2R} k_k; k_k + q_k; p_k + q_k T_{SSC}^R(k_k; q_k); \quad (A3)$$

and nally

$$T_{TSC}^R(p_k; q_k) = \frac{1}{4^{2V_F}} \ln \frac{1}{!} \int_{D_2} dk_k g_{1R} k_k; k_k + q_k; p_k g_{2R} k_k; k_k + q_k; p_k + q_k T_{TSC}^R(k_k; q_k); \quad (A4)$$

The anomalous dimension used in our RG equations for the renormalized form factors is given by<sup>15</sup>

$$(p_k; ! ) = \frac{1}{32^{4V_F^2}} \int_{D_5} dk_k dq_{1k} [2g_{1R} (k_k + p_k + q_{1k}; k_k; q_{1k})g_{1R} p_k; q_{1k}; k_k + 2g_{2R} p_k; q_{1k}; k_k + p_k + q_{1k} g_{2R} k_k; k_k + p_k + q_{1k}; q_{1k} g_{1R} p_k; q_{1k}; k_k g_{2R} k_k; k_k + p_k + q_{1k}; q_{1k} g_{2R} (p_k; q_{1k}; k_k + p_k + q_{1k})g_{1R} k_k; k_k + p_k + q_{1k}; p_k ]; \quad (A5)$$

## APPENDIX B

Considering the symmetries obeyed by the coupling functions we get the symmetrized ( ) renormalized form factors whose counterterms  $T_i^R$  are given by

$$T_{CDW}^R(p_k; q_k) = \frac{1}{4^{2V_F}} \ln \frac{1}{!} \int_{D_1} dk_k 2g_{1R} k_k; p_k q_k; p_k g_{2R} k_k; p_k q_k; k_k q_k T_{CDW}^R(k_k; q_k); \quad (B1)$$

$$T_{SDW}^R(p_k; q_k) = \frac{1}{4^{2V_F}} \ln \frac{1}{!} \int_{D_1} dk_k g_{2R} k_k; p_k q_k; k_k q_k T_{SDW}^R(k_k; q_k); \quad (B2)$$

$$T_{SSC}^R(p_k; q_k) = \frac{1}{4^{2V_F}} \ln \frac{1}{!} \int_{D_2} dk_k g_{1R} k_k; k_k + q_k; p_k + g_{2R} k_k; k_k + q_k; p_k + q_k T_{SSC}^R(k_k; q_k); \quad (B3)$$

and nally

$$T_{TSC}^R(p_k; q_k) = \frac{1}{4^{2V_F}} \ln \frac{1}{!} \int_{D_2} dk_k g_{1R} k_k; k_k + q_k; p_k g_{2R} k_k; k_k + q_k; p_k + q_k T_{TSC}^R(k_k; q_k); \quad (B4)$$

## APPENDIX C

In this appendix we will present all RG equations up to two-loop for the one-dimension case. For the quasi-particle weight we get simply

$$! \frac{d \ln Z}{d!} = \frac{1}{4^{2V_F^2}} g_{1R}^2 + g_{2R}^2 - g_{1R} g_{2R} \quad (C1)$$

In 1D the following equations for the renormalized coupling functions reduce simply to

$$\frac{dg_{1R}}{d!} = \frac{g_{1R}^2}{v_F} + \frac{g_{1R}^3}{2 v_F^2} \quad (C 2)$$

$$\frac{dg_{2R}}{d!} = \frac{g_{1R}^2}{2 v_F} + \frac{g_{1R}^3}{4 v_F^2} \quad (C 3)$$

Finally, the renormalized form factors are much simpler and they are now given by

$$\frac{dT_{CDWR}}{d!} = \frac{1}{2 v_F} (2g_{1R} - g_{2R}) T_{CDWR} + T_{CDWR} \quad (C 4)$$

$$\frac{dT_{SDWR}}{d!} = \frac{g_{2R}}{2 v_F} T_{SDWR} + T_{SDWR} \quad (C 5)$$

$$\frac{dT_{SSCR}}{d!} = \frac{1}{2 v_F} (g_{1R} + g_{2R}) T_{SSCR} + T_{SSCR} \quad (C 6)$$

$$\frac{dT_{TSCR}}{d!} = \frac{1}{2 v_F} (g_{2R} - g_{1R}) T_{TSCR} + T_{TSCR} \quad (C 7)$$

Consequently, the 1D resulting susceptibilities are now determined by

$$\frac{d\chi_a}{d!} = \frac{1}{2 v_F} (\chi_a)^2 \quad (C 8)$$

where  $a = CDW ; SDW ; SSC ; TSC$ .

---

Electronic address: eberth@iconp.org

- <sup>1</sup> A. Damascelli, D. H. Lee, Z. X. Shen, J. Electron Spectr. Relat. Phenom. 117-118, 165 (2001).
- <sup>2</sup> A. G. Loeser et al., Science 273, 325 (1996).
- <sup>3</sup> D. S. Marshall et al., Phys. Rev. Lett. 76, 4841 (1996).
- <sup>4</sup> H. Ding et al., Nature 382, 51 (1996).
- <sup>5</sup> P. W. Anderson, Science 235, 1196 (1987).
- <sup>6</sup> J. Voit, Rep. Prog. Phys. 58, 977 (1995).
- <sup>7</sup> E. H. Lieb and F. Y. Wu, Phys. Rev. Lett. 20, 1445 (1968).
- <sup>8</sup> J. Gonzalez, F. Guinea, and M. A. H. Vozmediano, ibid 79, 3514 (1997); D. Zanchi and H. J. Schulz, Phys. Rev. B 61, 13609 (2000); N. Dupuis, Int. J. Mod. Phys. B 14, 379 (2000); J. Gonzalez, Phys. Rev. B 63, 045114 (2001); P. Kopietz and T. Busche, Phys. Rev. B 64, 155101 (2001); B. Binz et al., Eur. Phys. J. B. 25, 69 (2002); A. A. Katanin and A. P. Kampf, Phys. Rev. B 68, 195101 (2003); T.

- Baier et al., Phys. Lett. B 605, 144 (2005).
- <sup>9</sup> C. J. Halboth and W. Metzner, Phys. Rev. B 61, 7364 (2000).
- <sup>10</sup> C. Honerkamp, M. Salmhofer, N. Furukawa, and T. M. Rice, Phys. Rev. B 63, 035109 (2001).
- <sup>11</sup> A. T. Zheleznyak, V. M. Yakovenko and I. E. Dzyaloshinskii, Phys. Rev. B 55, 3200 (1997).
- <sup>12</sup> F. V. Abreu and B. Doucot, Europhys. Lett. 38, 533 (1997).
- <sup>13</sup> J. Solyom, Adv. Phys. 28, 202 (1979).
- <sup>14</sup> H. Freire, E. Corrêa and A. Ferraz, arXiv cond-mat/0506682.
- <sup>15</sup> H. Freire, E. Corrêa and A. Ferraz, Phys. Rev. B 71, 165113 (2005).